

# UDT 2026 - Unlocking the Future of Underwater Surveillance with Ultra-Sensitive Wideband Electrometers

Gary Bagot, Sales Director, ELWAVE, Carquefou, France

Pierre Tuffigo, CEO, ELWAVE, Carquefou, France

Ultra-sensitive wideband electrometers introduce a complementary physical observable for underwater surveillance based on quasi-static electric field detection. This paper presents the ESENSE electrometer product range, developed following earlier work on active electric sensing, and details its intrinsic performance. We establish a theoretical framework for underwater electric detection and classification and derive realistic operational detection ranges for various target classes, including UUVs, USVs, vessels and submarines. These theoretical predictions are then compared with sea trial results (including NATO REPMUS 2025), demonstrating strong agreement between modeled and measured detection envelopes. Finally, two operational use cases are examined: harbor protection against kamikaze UUV threats and Anti-Submarine Warfare (ASW). Together, these results illustrate how ultra-sensitive wideband electrometry expands the underwater detection spectrum and strengthens multi-physics maritime surveillance architectures.

## 1 Introduction

ELWAVE's technological journey began in 2018 with the ambition to valorize the academic research conducted since early 2000's by its scientific partner the IMT Atlantique University on the active electric sense. Through a biomimicry approach, the aim was to reproduce the capability of some tropical fishes which generate a weak electric field into water and which sense its perturbations with extreme precision, enabling navigation, object detection and communication in highly cluttered environment. To do so the CEDAR technology (Controlled Electric Detection And Ranging) was developed to power EPULSE sensors product range and demonstrated unique underwater perception capabilities like non-metallic buried mines or combat diver detection [1].

Pushing the CEDAR® technology to its limits in terms of detection range through injecting more power and increasing its sensitivity revealed new insights. These same innovations required for active sensing (EPULSE), with extreme low-noise electronics, provided the foundation for the ultra-high performance passive electrometers ESENSE far exceeding the state-of-the-art and opening the door to long range detection and characterization of surface and underwater powered target's electrical signatures.

## 2 ESENSE: ultra-high performance underwater electrometers

### 2.1 Key technical features

The ESENSE product range is has an architecture with 3 components available in 300m and 6000m pressure housing, as well as OEM versions:

- The electrodes, made of robust titanium electrodes covered potentially covered with a specific coating depending on the requirements, which operate by pair to measure the electric potential gradient
- A processing unit with data storage capability and ethernet communication encapsulated into a 300m or 6000m depth rated system version (power consumption about 10W) or, alternatively, the OEM version, only PCBs with serial data output (power consumption about 1W)

As illustrated by the **Fig. 1**, in a 3 orthogonal axis configuration, ESENSE will measures the total electric field

( $E_T$ ) as follow:

$$E_T = \sqrt{E_x^2 + E_y^2 + E_z^2}$$

With:

$E_T$ , the total electric field in Volt/meter

$E_x$ , the electric field measured along the X axis between the electrode X1 (measurement of the tension  $V_{X1}$  in Volt) the electrode X2 (measurement of the tension  $V_{X2}$  in Volt), separated by a distance  $D_{X1-X2}$ , the baseline  $L$ , calculated as below:

$$E_x = \frac{V_{X1} - V_{X2}}{D_{X1-X2}}$$

and similarly for the y and z components.

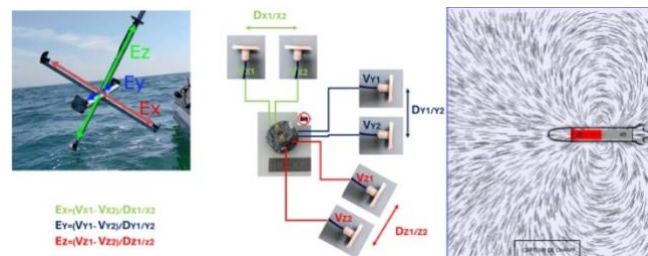


**Fig. 1** - ESENSE illustration. Left image: 3-axis configuration at sea of the 300m depth rated version. Middle image: 3-axis OEM configuration. Right image: sensor main components.

Furthermore, ESENSE integrates auto-calibration functionality. At sensor initialization, ESENSE will check for any bias in between each pair of electrodes and electronically compensate them to maintain precision and accuracy of the measurements, limiting manufacturer recalibration. This process takes less than one second.

The sensors, available in 300 m and 6000 m system configurations, are supplied with the OWLIA software featuring real-time monitoring and replay capabilities for multi-axis electric field measurements. The software integrates advanced signal processing tools, including FFT analysis, spectrogram visualization, PSD estimation, and demodulation functions for detailed signal characterization.

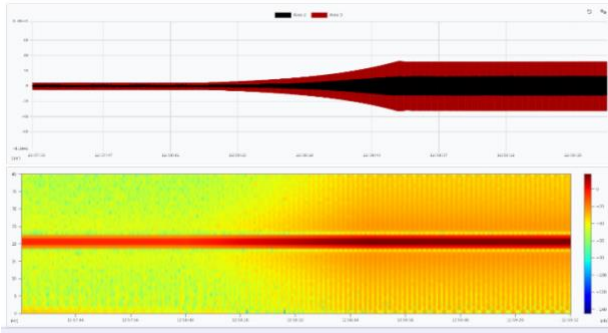


**Fig. 2** - OWLIA user interface software by ELWAVE. Upper box: Electric fields measured by 2 pairs of electrodes. Lower box: spectrogram showing a strong electric field at 20Hz.

## 2.2 Theoretical Detection Range of ESENSE electrometer

### 2.2.1 Intrinsic performance of ESENSE Electrometers

ESENSE is a wideband (DC–2 kHz) differential electrometer designed to measure low-frequency electric field gradients in conductive marine environments. The sensor measures potential difference between electrodes separated by a defined baseline.

Intrinsic noise is expressed as voltage spectral density (nV/ $\sqrt{\text{Hz}}$  RMS). The equivalent electric field spectral density is obtained by dividing voltage noise by baseline length.

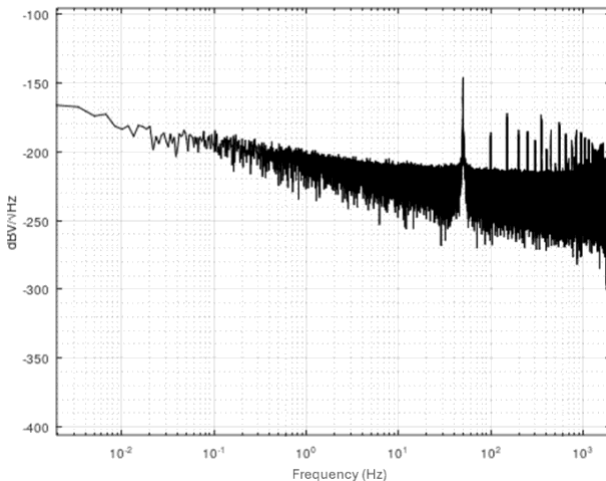


**Fig. 3** - ESENSE Ultra-sensitive wideband electrometer noise spectral density performance. No numerical filter used, only raw data acquisition over 10 minutes in a protected environment.

Measured intrinsic noise levels over a 10-minute acquisition without filtering are shown below. These values are expressed in spectral density form, consistent with standard electrometry practice [3; 6].

**Table 1.** ESENSE Intrinsic Noise Spectral Density (1 m Baseline)

| Frequency (Hz) | Voltage Noise (nV/ $\sqrt{\text{Hz}}$ ) | Equivalent Field Noise (nV/m/ $\sqrt{\text{Hz}}$ ) |
|----------------|---|--|
| 0.01           | 0.6                                     | 0.6  |
| 0.1            | 0.5                                     | 0.5  |
| 1              | 0.1                                     | 0.1  |
| 1–2000         | <0.1                                    | <0.1   |

For the purpose of detection range modeling, the following reference conditions are adopted throughout this section:

- Seawater conductivity: 4 S/m
- Environmental noise:  $-165 \text{ dBV/m}/\sqrt{\text{Hz}}$
- Equivalent noise:  $5.62 \text{ nV/m}/\sqrt{\text{Hz}}$

- Detection band: DC–10 Hz
- Signal-to-noise ratio: SNR = 2
- Baseline: 1 m
- Sensor and source located mid-water
- Water depth larger than detection range

Under these reference conditions, a 1 A·m electric dipole corresponds to approximately 150 m detection range ( $r$ ). All subsequent scaling factors are applied relative to this baseline configuration.

### 2.2.2 Propagation Model in Conductive Seawater

At low frequencies (DC–10 Hz), electromagnetic propagation in seawater is governed by quasi-static diffusion theory. For conductivity  $\sigma \approx 4 \text{ S/m}$ , skin depth is approximately 800 m at 1 Hz and 250 m at 10 Hz. Since typical detection distances remain well below these values, the quasi-static approximation is valid.

The electric field generated by an equivalent dipole moment  $p(\text{A}\cdot\text{m})$  is given by classical theory [3; 4]:

$$E(r) = \frac{p}{2\pi\sigma r^3}$$

For  $\sigma = 4 \text{ S/m}$ , this yields:

$$E(r) = \frac{p}{2\pi\sigma r^3}$$

$$E_{10} \approx 40 \text{ } \mu\text{V/m per A}\cdot\text{m}$$

This conversion is used consistently throughout the detection analysis.

### 2.2.3 Representative Target Source Levels

Open-access quantitative electric signatures for naval platforms remain limited, likely due to operational sensitivity. The values adopted here are engineering estimates derived from corrosion current modeling, ICCP systems, and equivalent dipole reconstructions reported in electromagnetic signature studies [7; 8].

These source levels represent steady-state nominal operation and do not include maneuver-induced amplification, which is treated separately.

**Table 2.** Typical Dipole Moments and Electric Field at 10 m

| Target Type                                       | Dipole Moment (A·m) | Field at 10 m ( $\mu\text{V/m}$ ) |
|---|---------------------|-----------------------------------|
| Small UUV   | 0.1 – 1             | 4 – 40                            |
| Mid-size UUV (5 m composite hull)                 | 0.5 – 3             | 20 – 120                          |
| Small USV   | 1 – 5               | 40 – 200                          |
| Submerged metallic hull (submarine configuration) | 3 – 50              | 120 – 2000                        |
| Large ICCP vessel                                 | 20 – 200            | 800 – 8000                        |

### 2.2.4 Steady-State Detection Range

Using the propagation model and reference offshore parameters:

$$r = \left( \frac{p}{2\pi\sigma \cdot \text{SNR} \cdot E_{noise}} \right)^{1/3}$$

Steady-state detection ranges are computed below (for one single sensor).

**Table 3.** Steady-State Detection Range ( $\sigma = 4$  S/m,  $-165$  dBV/m/ $\sqrt{\text{Hz}}$ , SNR = 2, 1 m Baseline)

| Target Type             | Detection Range (m)<br><i>One single sensor</i> |
|-------------------------|---|
| Small UUV               | 70 – 150  |
| Large Kamikaze UUV      | 120 – 220                                       |
| Submerged metallic hull | 220 – 550                                       |
| Large ICCP vessel       | 380 – 950                                       |

### 2.2.5 Manoeuvre and Transient Amplification

Operational manoeuvring may increase effective dipole moment due to propulsion load variation, heading changes, transient current imbalance, and wake magnetohydrodynamic effects. Amplification factors between  $\times 3$  and  $\times 5$  are consistent with electromagnetic modelling studies [7].

Since detection range scales as:  $r \propto p^{\frac{1}{3}}$ , transient events extend detection range predictably.

**Table 4.** Detection range under transient conditions ( $\sigma = 4$  S/m,  $-165$  dBV/m/ $\sqrt{\text{Hz}}$ , SNR = 2, 1 m Baseline)

| Target Type             | Steady (m) | Moderate $\times 3$ (m) | Strong $\times 5$ (m) |
|-------------------------|------------|-------------------------|-----------------------|
| Small UUV               | 70–150     | 100–215                 | 120–260               |
| Large Kamikaze UUV      | 120–220    | 175–315                 | 205–375               |
| Submerged metallic hull | 220–550    | 315–790                 | 375–950               |
| Large ICCP vessel       | 380–950    | 540–1370                | 650–1650              |

### 2.2.6 Frequency Band Dependence

Although ESENSE operates from DC to 2 kHz, detection range is governed by conductive attenuation at higher frequencies. Skin depth decreases significantly above 10 Hz. When detection distance approaches skin depth, exponential attenuation reduces effective range:

$$E(r) \propto \frac{1}{r^3} e^{-r/\delta}$$

DC–10 Hz remains fully quasi-static for the detection ranges considered. Higher frequencies contribute primarily to classification capability rather than long-range detection.

**Table 5.** Detection range scaling by frequency

| Frequency Band | Detection Range Factor |
|----------------|------------------------|
| DC–0.1 Hz      | 0.95                   |
| 0.1–1 Hz       | 1.00                   |
| 1–10 Hz        | 1.00                   |
| 10–50 Hz       | 0.6 – 0.8              |
| 50–200 Hz      | 0.3 – 0.5              |
| 200 Hz–2 kHz   | 0.1 – 0.3              |

### 2.2.7 Environmental and Geometric Scaling Factors

Detection range scales predictably with environmental noise, conductivity, baseline length, and water depth. These factors modify measurable signal-to-noise ratio but do not alter source strength.

ESENSE detection range related to environmental noise follows:

$$r \propto E_{noise}^{-1/3}$$

**Table 6.** Detection Range Scaling with Environmental Noise (Reference  $-165$  dBV/m/ $\sqrt{\text{Hz}}$ , extrapolated form [2])

| Noise Level (dBV/m/ $\sqrt{\text{Hz}}$ ) | Equivalent (nV/m/ $\sqrt{\text{Hz}}$ ) | Typical Environment | Detection Range Factor |
|--|--|---------------------|------------------------|
| -180                                     | 1.0                                    | Quiet offshore      | 1.44                   |
| -165                                     | 5.62                                   | Offshore reference  | 1.00                   |
| -150                                     | 31.6                                   | Coastal waters      | 0.69                   |
| -135                                     | 178                                    | Harbor / industrial | 0.48                   |

ESENSE detection range related to water conductivity follows:

$$r \propto \sigma^{-1/3}$$

**Table 7.** Detection range scaling with conductivity (Ref.: 4 S/m)

| Conductivity (S/m) | Typical Region     | Detection Range Factor |
|--------------------|--------------------|------------------------|
| 6                  | High salinity seas | 0.87                   |
| 4                  | Atlantic offshore  | 1.00                   |
| 2                  | Baltic Sea         | 1.26                   |
| 0.8                | Estuarine waters   | 1.71                   |

Increasing ESENSE inter-electrode baseline significantly improves the detection range as below:

**Table 8.** Detection range scaling with baseline length (Ref.: 1 m)

| Baseline (m) | Detection Range Factor |
|--------------|------------------------|
| 1            | 1.00                   |
| 2            | 1.26                   |
| 5            | 1.71                   |
| 10           | 2.15                   |

The water depth and the relative vertical distance between ESENSE and the target influence the detection as below.

**Table 9.** Detection Range Scaling Due to Water Depth and Geometry (Reference Deep Water, Mid-Water Configuration)

| Configuration           | Physical Effect                   | Detection Range Factor |
|-------------------------|-----------------------------------|------------------------|
| Deep water, mid-water   | Unbounded medium assumption valid | 1.00                   |
| Sensor near surface     | Partial vertical confinement      | 1.05 – 1.15            |
| Sensor near seabed      | Sediment interaction              | 1.00 – 1.10            |
| Shallow shelf (10–30 m) | Horizontal confinement            | 1.10 – 1.30            |

## 3 ESENSE performances measured at sea

In this section, the ESENSE sea trials are compared with the theoretical detection ranges previously established using the dipole propagation model.

The objective is to verify that real-world operational measurements remain consistent with the conductivity, noise, and transient scaling laws described earlier.

The dataset includes controlled validation experiments as well as operational deployments conducted during NATO REPMUS 2025 exercises.

During REPMUS, ESENSE was remotely operated in real time, integrated into unmanned surface vehicle (USV), a French Navy RHIB and a small boat and evaluated in realistic ISR conditions.

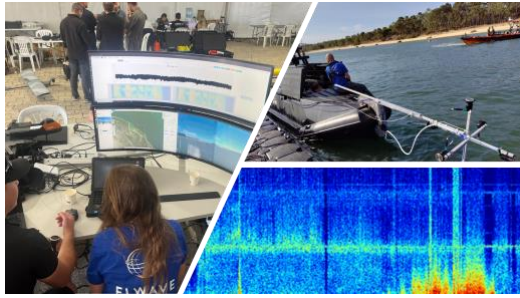


Fig. 4 - ESENSE sensor in 3 axis configurations mounted on a USV and data QA/QC from remote control centre NATO REPMUS 2025.

Table 10. ESENSE sea trials detection range vs theoretical envelope (considering distance inter-electrode L=1 m)

| Vehicle source               | Measured seawater $\sigma$ (S/m) | Measured noise (dBV/m/ $\sqrt{\text{Hz}}$ ) | Theoretical detection range Envelope (m) | Observed Detection (m) |
|------------------------------|----------------------------------|---|--|------------------------|
| UUV                          | 0.8                              | -180  | 180 - 240                                | 147                    |
| UUV + MAD target             | 3.5                              | -150  | 420 - 520                                | 485                    |
| Submarine (NATO REPMUS 2025) | 6                                | -150  | 650 - 1050                               | up to ~1000m           |
| USV (NATO REPMUS 2025)       | 6.6                              | -150  | 20 - 35                                  | 25m                    |

In addition to detection, using high precision spectral analysis, the system successfully tracked another USV deploying an ROV and enabled discrimination between the electric signature of the ESENSE carrier USV, the target USV, and the ROV deployed by the target.

This demonstrated not only detection capability but also signature separation and classification potential in multi-platform dynamic environments.

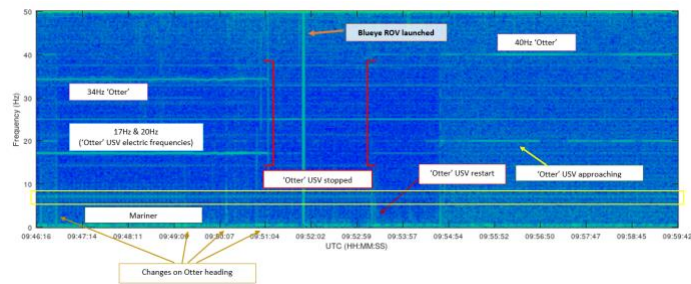


Fig. 5 ESENSE Spectrogram of USV and ROV Deployment Operations

The consistency between measured tracking distances and the predicted theoretical envelopes for a diverse set of vehicles and environments confirms that ESENSE achieves the expected and theoretical detection ranges and spectral classification performances.

#### 4 Use Case 1: Counter-UUV - ESENSE barrier for naval base and vessel protection

Ukrainian war has highlighted the new threats of kamikaze UUVs targeting military ports. We examine here a highly efficient and scalable counter-UUV solution configuration in which a permanent ESENSE seabed network protects a several nautical miles harbour approach against a hostile UUV

navigating within the thermocline to minimize acoustic detectability.

The kamikaze UUV characteristic are:

- Dipole moment:  $p = 2 \text{ A} \cdot \text{m}$
- Navigation depth: 1 m immersion
- Navigation speed: 5m/s
- Water depth: 30 m
- Seawater conductivity: 4 S/m
- Seabed conductivity: 1 S/m
- Environmental noise: 5 nV/m RMS
- Detection threshold:  $\text{SNR} = 1.5$
- ESENSE electrodes 1m above the seabed
- 3-layer electric field propagation model

#### 4.1.1 Barrier Architecture

The defensive barrier consists of:

- 3 parallel seabed lines, spaced 100 m apart
- Sensors spaced every 250 m along each line

This corresponds to 12 sensors per km (4 per line  $\times$  3 lines).

We consider an effective detection radius of 180 m per sensor, the configuration ensures overlapping coverage and eliminates blind corridors.

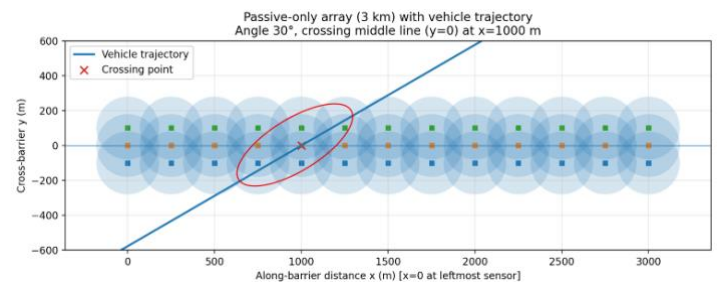


Fig. 6 Barrier of ESENSE subsea stations over 3 lines for Kamikaze UUV detection by 6 sensors within the red ellipse

#### 4.1.2 Detection Mechanism

As the UUV crosses the barrier, the six closest sensors generate the dominant electric response. Detection occurs when the measured field exceeds  $\text{SNR} = 1.5$  relative to the 5 nV/m noise floor. Because multiple sensors cross threshold in a coherent temporal sequence, false alarms from isolated disturbances are mitigated.

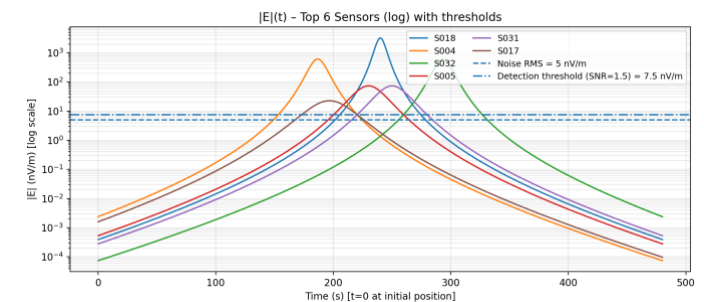


Fig.7 Electric Field measurements evolution by the 6 ESENSE sensors showing threshold crossings

#### 4.1.3 Network-Level Tracking

The ESENSE barrier operates as a cooperative sensing mesh. Two indicators are used:

- Temporal increase in the number of detecting sensors

- A weighted network detection score (*algorithm confidential*)
- A probabilistic presence map (warm colour = high probability) is updated in real time and feeds a specific tracking algorithms (*algorithm confidential*), enabling trajectory estimation without relying on raw amplitude alone.

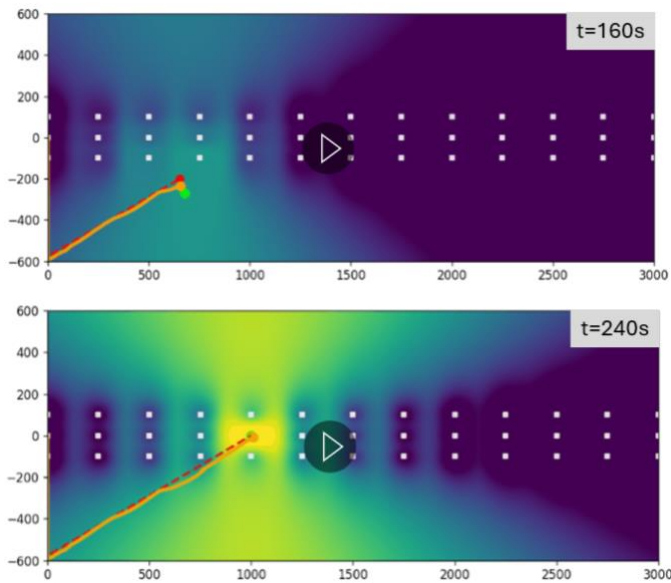


**Fig. 8** Simulation of a kamikaze UUV detection and tracking by the ESENSE barrier. Red line is the true UUV route, Green dot is the instantaneous UUV localisation by the sensors array, the orange line is the reconstructed UUV route

#### 4.1.4 Operational Significance

This use case illustrates the highly operational relevance of ESENSE for protecting sensitive maritime infrastructure against emerging underwater threats. A kamikaze UUV navigating close to sea surface as a very low detectable acoustic signature, especially in noisy port environments where shipping traffic, reflections, and stratification degrade sonar performance. In such conditions, acoustic barriers are inefficient.

The ESENSE barrier operates on a different physical observable: the quasi-static electric field generated by the vehicle's hull polarization and propulsion currents. This signal does not depend on cavitation or acoustic emission and remains detectable even at very low speed.

The distributed seabed configuration ensures early detection, spatial coherence, and robust tracking before the intruder reaches critical assets.

The duration of the continuous alert and tracking is around 200s giving significant reaction time to detect, locate and then neutralize the intruder.

ESENSE offers a discrete operating mode, immune to acoustic masking strategies, and scalable network deployment.

It provides a unique high efficiency counter-UUV layer for the protection of naval bases, military ports, and high-value coastal sites facing modern kamikaze submarine threats.

## 5 Use Case 2: Anti-Submarine Warfare – ESENSE electrobuoys and thin-line array

### 5.1.1 Current ASW Limitations

Modern Anti-Submarine Warfare (ASW) relies on active sonar, passive acoustics, and magnetic anomaly detection (MAD).

Active sonar provides range but is highly sensitive to environmental conditions. In shallow waters, multipath propagation, thermoclines, and strong bottom reverberation, particularly over hard seabed, can significantly degrade performance [9].

Passive acoustic detection depends on radiated noise; however, modern submarines are increasingly quiet, especially diesel-electric platforms operating on battery power at low speed in littoral environments [10]. MAD systems detect disturbances of the Earth's magnetic field caused by ferromagnetic mass, but detection range is inherently limited and typically remains within a few hundred meters [11]. All three approaches target signatures that modern submarines are specifically engineered to minimize.

### 5.1.2 Electric Field Detection as a New Observable

ESENSE introduces a complementary detection channel based on quasi-static electric fields generated by hull polarization, ICCP systems, corrosion currents, and propulsion-related imbalances.

Passive electric detection:

- does not rely on cavitation or radiated sound,
- remains effective at very low speed,
- is not affected by thermoclines and acoustic shadow zones,
- operates passively and covertly.

Unlike acoustic and magnetic signatures, the submarine's electric emissions are generally not optimized for stealth.

The operational (NATO REPMUS 2025) evaluation performed with a single sensor deployed 1m below the sea has given a detection range of a submarine of the order of one kilometer.

We consider a length of the electric measures section of 100m, with ESENSE electrodes (OEM version) every 5m, deployed vertically (electrobuoys). The source is 50A.m. The submarine navigates 100m below the sea surface.

In this use case, we consider a quiet offshore electric environment, the electric noise is  $1\text{nV/m}/\sqrt{\text{Hz}}$ .

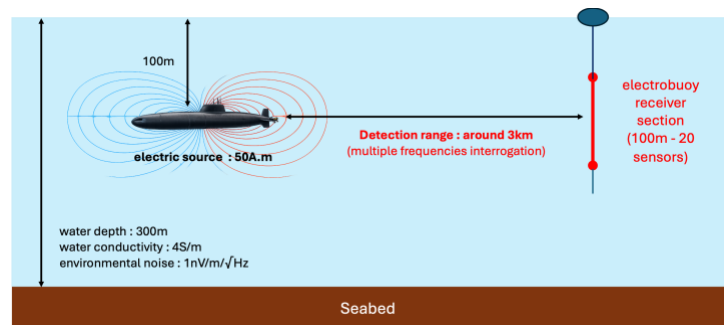


**Fig. 9** submarine detection range with passive electric sensors array

The array offers two benefits: the rejection of common and coherent environmental noise and the use of narrow-band lock-in algorithms.

Considering several discrete frequencies interrogation, the detection range of this vehicle is around 3km.

Here below, we evaluate the detection range as a function of the seawater conductivity from 1S/m (Baltic Sea) to 7S/m (Persian Gulf):

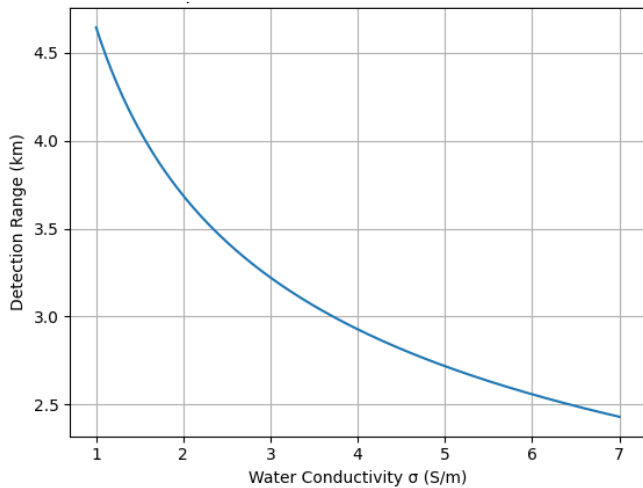


Fig. 10 Submarine detection range as a function of the seawater conductivity

### 5.1.3 Operational Relevance

This capability is particularly relevant in shallow or acoustically complex environments such as the Baltic Sea or Persian Gulf, where stratification, high ambient noise, and bottom reverberation reduce acoustic effectiveness.

Electric field detection is far less sensitive to these constraints and provides an independent observable when acoustic performance degrades.

The integration of ESENSE into buoys, thin-line arrays towed by UUVs or USVs or seabed nodes offers a highly effective complementary detection, classification, identification and tracking capabilities complementary to existing acoustics systems.

In a domain historically dominated by acoustics, underwater electric field sensing represents a complementary and potentially decisive addition to modern ASW architectures.

The rapid adoption of ESENSE by any navy would enable it to build a comprehensive database of adversary submarine electric signatures, thereby securing critical operational advantage over its competitors.

## 6 Conclusion

ELWAVE's ultra-sensitive wideband electrometry opens a new frontier in underwater surveillance.

Validated by both modeling and sea trials, ESENSE underwater electric field sensors have demonstrated operational detection ranges from several hundred meters to kilometer scales.

By introducing an independent physical observable largely unaddressed by modern stealth optimization, electric field sensing complements acoustics and strengthens detection resilience.

As navies move toward multi-physics architectures, early integration of wideband electrometers will be key to building the signature databases and capabilities that define the future of underwater security.

## Acknowledgements

The authors thank the UDT Technical Conference Committee and the reviewers for their constructive feedback. Special appreciation is extended to Dr. Olav Holberg (FFI) for his support and insights. The ELWAVE team is also gratefully acknowledged for its contribution to this work.

## References

- [1] Q. Delplanque, L. Ifrek, F. Boyer, V. Lebastard. Detection method in electrically conductive media. Patent N° FR20230011308A. 2020
- [2] A. D. Chave, J. H. Filloux. Observation and interpretation of the seafloor vertical electric field. *Journal of Geophysical Research*, 1985.
- [3] Jackson, J. D. (1998). *Classical Electrodynamics* (3rd ed.). Wiley.
- [4] Wait, J. R. (1982). *Geo-Electromagnetism*. Academic Press.
- [5] Chave, A. D., & Cox, C. S. (1982). Controlled electromagnetic sources for measuring electrical conductivity beneath the oceans. *Journal of Geophysical Research*.
- [6] Ward, S. H., & Hohmann, G. W. (1988). *Electromagnetic methods in applied geophysics*. SEG.
- [7] Sun et al. (2020). Electromagnetic modeling of underwater vehicles. *IEEE Transactions on Magnetics*.
- [8] Wang et al. (2018). Electric signature modeling of marine vessels. *Ocean Engineering*.
- [9] Urick, R. J. (1983). *Principles of Underwater Sound* (3rd ed.). McGraw-Hill.
- [10] Richardson, W. J., Greene, C. R., Malme, C. I., & Thomson, D. H. (2001). *Marine Mammals and Noise*. Academic Press.
- [11] Campbell, W. H. (2006). *Introduction to Geomagnetic Fields* (2nd ed.). Cambridge University Press.

## Author/Speaker Biographies

Gary BAGOT, Partner and Sales Director, hydrographer with previous experience in the French Navy, offshore industry and EXAIL.

Pierre TUFFIGO, CEO and founder of ELWAVE, optronics engineer with previous experience at THALES and the French Defence Procurement agency (DGA).